Entanglement features in the Kondo Model

Anirban Mukherjee* and Siddhartha Lal†

Department of Physical Sciences, IISER Kolkata

N.S. Vidhyadhiraja‡

Theoretical Sciences Unit, JNCASR, Bangalore

Arghya Tarapdher§

Physics Department and Centre for Theoretical Studies, IIT Kharagpur

(Dated: June 11, 2020)

Abstract

To be written...

INTRODUCTION

Motivation for the work For an antiferromagnetic Kondo coupling, a Kondo cloud is formed via the entanglement between the impurity spin and conduction electrons. On the other hand, for a ferromagnetic Kondo coupling, the impurity spin disentangles from the conduction electrons. In the present work, we aim to study the interplay between electronic correlations in the neighbourhood of the Fermi surface (FS) and fermion sign exchanges in the many-particle wavefunction in shaping the entanglement between the Kondo cloud and the impurity spin. This will help in advancing our understanding of the quantum liquid that comprises the Kondo cloud. We will employ a combination of entanglement-based and Green function-based measures to unravel the various features of the quantum liquid.

THE MODEL

The Kondo model [1, 2] describes the coupling between a magnetic quantum impurity localized in real space with a bath of conduction electrons

$$\hat{H} = \sum_{\mathbf{k}\sigma} \epsilon_{\mathbf{k}} \hat{n}_{\mathbf{k}\sigma} + \frac{J}{2} \sum_{\mathbf{k},\mathbf{k}'} \mathbf{S} \cdot c^{\dagger}_{\mathbf{k}\alpha} \boldsymbol{\sigma}_{\alpha\beta} c_{\mathbf{k}'\beta} \ . \tag{1}$$

Here, we consider a 2D electronic bath $\epsilon_{\mathbf{k}} = -2t(\cos k_x + \cos k_y)$ with the Fermi energy $E_F = \mu$. J is the Kondo scattering coupling between the impurity and the conduction electrons. An important feature of the Kondo coupling is the two different classes of scattering processes: one involving spin-flip scattering processes for the bath electrons ($c^{\dagger}_{\mathbf{k}\uparrow} c_{\mathbf{k}'\downarrow} + h.c.$), and the other not (i.e., simple potential scattering processes). In the antiferromagnetic regime $J > 0$, the spin-flip scattering processes generates quantum entanglement between the impurity spin and a macroscopic number of bath electrons (called the "Kondo cloud"), resulting in the complete screening of the impurity via the formation of a singlet spin state. It is clear that the dynamical Kondo cloud corresponds to an effective single spin-1/2, such that the screening is an example of macroscopic quantum entanglement arising from electronic correlations. It is the nature of this entanglement, and the underlying quantum liquid that forms the Kondo cloud, that we seek to learn more of.

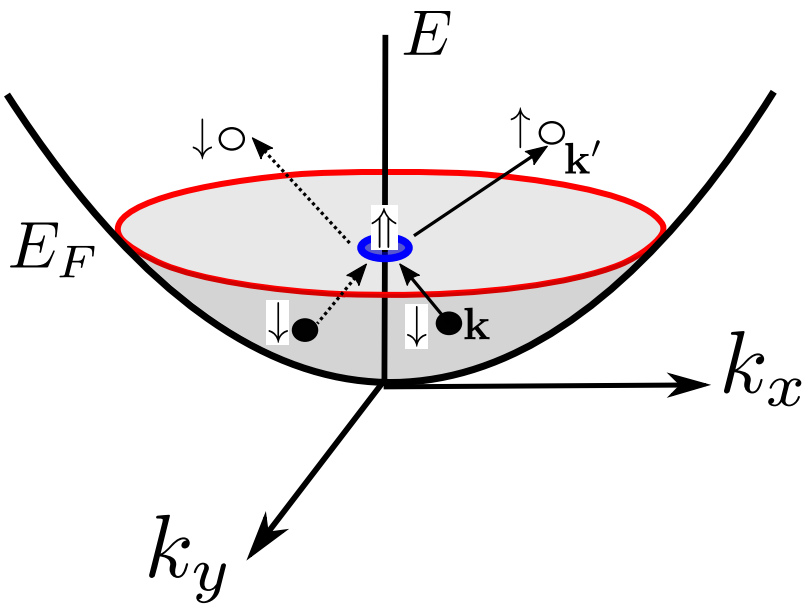

FIG. 1. The Kondo model is composed of a two-dimensional conduction electron bath (Fermi liquid) coupled to a magnetic impurity via a spin-flip (solid) / non spin-flip (dashed) scattering coupling.

URG THEORY FOR THE KONDO MODEL

In constructing an effective low-energy theory for the Kondo singlet, we employ the unitary RG formalism to the Kondo model such that electronic states from the non-interacting conduction bath are stepwise disentangled, starting with the highest energy electrons at the bandwidth and eventually scaling towards the FS. While this aspect is similar to Anderson's poor man's scaling [2], we shall see that several other aspects of the unitary RG formalism are different from those adopted in the poor man's scaling approach. The electronic states are labelled in terms of the normal distance Λ from the FS and the orientation unit vectors (Fig.2) $\hat{s}$: $\mathbf{k}_{\Lambda\hat{s}} = \mathbf{k}_F(\hat{s}) + \Lambda\hat{s}$, where $\hat{s} = \frac{\nabla\epsilon_{\mathbf{k}}}{|\nabla\epsilon_{\mathbf{k}}|}|_{\epsilon_{\mathbf{k}}=E_F}$. The states are labelled as $|j, l, \sigma\rangle = |\mathbf{k}_{\Lambda_j\hat{s}}, \sigma\rangle, l := (\hat{s}_m, \sigma)$.

The Λ's are arranged as follows: $\Lambda_N > \Lambda_{N-1} > \ldots > 0$, where the electronic states farthest from FS Λ_N are disentangled first, eventually scaling towards the FS. This leads to the Hamiltonian flow equation

$$H_{(j-1)} = U_{(j)} H_{(j)} U_{(j)}^{\dagger} \ , \tag{2}$$

where the unitary operation $U_{(j)}$ is the unitary map at RG step j. $U_{(j)}$ disentangles all the

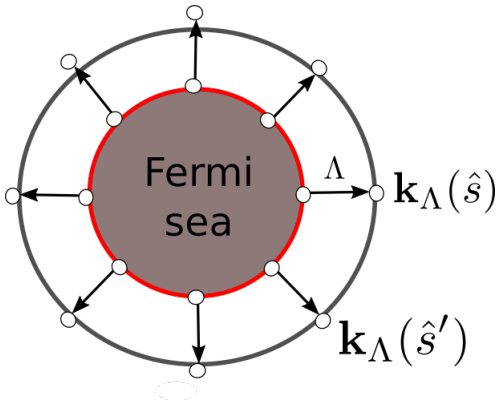

FIG. 2. Fermi surface geometry for a circular Fermi volume of non-interacting electrons in 2 spatial dimensions.

electronic states **AM$|\mathbf{k}_{\Lambda_j \hat{s}_m}, \sigma\rangle$AM** on the isogeometric curve and has the form[3]

$$U_{(j)} = \prod_l U_{j,l}, U_{j,l} = \frac{1}{\sqrt{2}}[1 + \eta_{j,l} - \eta^\dagger_{j,l}] \ , \tag{3}$$

where $\eta_{j,l}$ are electron-hole transition operators following the algebra

$$\{\eta_{j,l}, \eta^\dagger_{j,l}\} = 1 \ , \quad \left[\eta_{j,l}, \eta^\dagger_{j,l}\right] = 1 \ . \tag{4}$$

The transition operator can be represented in terms of the diagonal (H^D) and off-diagonal (H^X) parts of the Hamiltonian as follows

$$\eta_{j,l} = Tr_{j,l}(c^\dagger_{j,l} H_{j,l}) c_{j,l} \frac{1}{\hat{\omega}_{j,l} - Tr_{j,l}(H^D_{j,l} \hat{n}_{j,l}) \hat{n}_{j,l}} \ . \tag{5}$$

We note that in the numerator of the expression for $\eta_{j,l}$, the operator $Tr_{j,l}(c^\dagger_{j,l} H_{j,l}) c_{j,l} + h.c.$ is composed of all possible scattering vertices that modify the configuration of the electronic state $|j,l\rangle$. The generic forms of $H^D_{j,l}$ and $H^X_{j,l}$ are as follows

$$\begin{aligned} H^D_{j,l} &= \sum_{\Lambda \hat{s}, \sigma} \epsilon^{j,l} \hat{n}_{\mathbf{k}_{\Lambda \hat{s}}, \sigma} + \sum_\alpha \Gamma^{4,(j,l)}_\alpha \hat{n}_{\mathbf{k}\sigma} \hat{n}_{\mathbf{k}'\sigma'} + \sum_\beta \Gamma^{8,(j,l)}_\beta \hat{n}_{\mathbf{k}\sigma} \hat{n}_{\mathbf{k}'\sigma'} (1 - \hat{n}_{\mathbf{k}''\sigma''}) + \dots \ , \\ H^X_{j,l} &= \sum_\alpha \Gamma^2_\alpha c^\dagger_{\mathbf{k}\sigma} c_{\mathbf{k}'\sigma'} + \sum_\beta \Gamma^2_\beta c^\dagger_{\mathbf{k}\sigma} c^\dagger_{\mathbf{k}'\sigma'} c_{\mathbf{k}'_1\sigma'_1} c_{\mathbf{k}_1\sigma_1} + \dots \ . \end{aligned} \tag{6}$$

The operator $\hat{\omega}_{j,l}$ accounts for the quantum fluctuations arising from the non-commutativity between different parts of the renormalized Hamiltonian and has the following form [4]

$$\hat{\omega}_{j,l} = H^D_{j,l} + H^X_{j,l} - H^X_{j,l-1} \ . \tag{7}$$

Upon disentangling electronic states $\hat{s}, \sigma$ along a isogeometric curve at distance Λ_j, the following effective Hamiltonian $H_{j,l}$ is generated

$$H_{j,l} = \prod_{m=1}^{l} U_{j,m} H_{(j)} [\prod_{m=1}^{l} U_{j,l}]^{\dagger} \ . \tag{8}$$

****AM** And $H_{j,2n_j+1} = H_{(j-1)}$ is the Hamiltonian obtained after disentangling all the electronic states on the isogeometric curve j. Below we depict the different terms generated upon successive disentanglement of the states $|\mathbf{k}_{\Lambda_j \hat{s}_l}, \sigma\rangle$ on a given curve,

$$\begin{aligned}
H_{j,l+1} &= Tr_{j,l}(H_{(j,l)}) + \{c^{\dagger}_{j,l} Tr_{j,l}(H_{(j,l)} c_{j,l}), \eta_{j,l}\}\tau_{j,l}, \tau_{j,l} = \hat{n}_{j,l} - \frac{1}{2} \\
H_{j,l+2} &= Tr_{j,l+1}(Tr_{j,l}(H_{(j,l)})) + Tr_{j,l+1}(\{c^{\dagger}_{j,l} Tr_{j,l}(H_{(j,l)} c_{j,l}), \eta_{j,l}\}\tau_{j,l}) \\
&\quad + \{c^{\dagger}_{j,l+1} Tr_{j,l+1}(Tr_{j,l}(H_{(j,l)}) c_{j,l+1}), \eta_{j,l+1}\}\tau_{j,l+1} \\
&\quad + \{c^{\dagger}_{j,l+1} Tr_{j,l+1}(\{c^{\dagger}_{j,l} Tr_{j,l}(H_{(j,l)} c_{j,l}), \eta_{j,l}\} c_{j,l+1}), \eta_{j,l+1}\}\tau_{j,l}\tau_{j,l+1} \ . \\
H_{j,l+3} &= \ldots \text{terms with} \tau_{j,l}, \tau_{j,l+1}, \tau_{j,l+2} \ldots \\
&\quad + \ldots \text{terms with} \tau_{j,l}\tau_{j,l+1}, \tau_{j,l+1}\tau_{j,l+2}, \tau_{j,l}\tau_{j,l+2} \ldots \\
&\quad + \ldots \text{terms with} \tau_{j,l}\tau_{j,l+1}\tau_{j,l+2}.
\end{aligned} \tag{9}$$

Upon disentangling multiple electronic states placed in the tangential direction on a given momentum shell at distance Λ_j generates RG contribution from leading order scattering processes (terms multiplied with $\tau_{j,l}$, $\tau_{j,l+1}$, etc.) that goes as $Area/Vol = 1/L$ and higher order processes like terms multiplied with $\tau_{j,l}\tau_{j,l+1}$ that goes as $(Area)^2/Vol^2 = 1/L^2$, $\tau_{j,l}\tau_{j,l+1}\tau_{j,l+2}$ that goes as $(Area)^3/Vol^3 = 1/L^3$. Accounting for only the leading tangential scattering processes, as well as other momentum transfer processes along the normal direction $\hat{s}$, the renormalized Hamiltonian has the form

$$H_{(j-1)} = Tr_{j,(1,\ldots,2n_j)}(H_{(j)}) + \sum_{l=1}^{2n_j} \{c^{\dagger}_{j,l} Tr_{j,l}(H_{(j)} c_{j,l}), \eta_{j,l}\}\tau_{j,l} \ . \tag{10}$$

Here, $2n_j$ are the number of electronic states on the isogeometric curve at distance Λ_j, and $\tau_{j,l} = n_{j,l} - \frac{1}{2}$. **AM****

RESULTS

The unitary RG process generates the effective Hamiltonian's $\hat{H}_{(j)}(\omega)$'s for various eigen directions $|\Phi(\omega)\rangle$ of the $\hat{\omega}$ operator. Note the associated eigenvalue ω identifies a subspec-

trum in the interacting many body eigenspace. The form of $\hat{H}_{(j)}(\omega)$ is given by,

$$\hat{H}_{(j)}(\omega) = \sum_{j,l,\sigma} \epsilon_{j,l}\hat{n}_{j,l} + \frac{J^{(j)}(\omega)}{2} \sum_{\substack{j_1,j_2<j,\\ m,m'}} \mathbf{S}\cdot c^{\dagger}_{j_1,\hat{s}_m,\alpha}\boldsymbol{\sigma}_{\alpha\beta}c_{j_2,\hat{s}_{m'},\beta} + \sum_{\substack{a=N,\\ m=1}}^{j,n_j} J^{(a)}S^z s^z_{a,\hat{s},m}, \quad (11)$$

where $s^z_{l,\hat{s},m} = \frac{1}{2}(\hat{n}_{l,\hat{s}_m,\uparrow} - \hat{n}_{l,\hat{s}_m,\downarrow})$. The Kondo coupling RG equation for the RG steps(Appendix) has the form,

$$\frac{\Delta J^{(j)}(\omega)}{\Delta \log \frac{\Lambda j}{\Lambda_0}} = \frac{n_j (J^{(j)})^2 \left[(\omega - \frac{\hbar v_F \Lambda_j}{2})\right]}{(\omega - \frac{\hbar v_F \Lambda_j}{2})^2 - \frac{\left(J^{(j)}\right)^2}{16}} \quad (12)$$

AM where n_j is the no. of electronic states **AM Note that the denominator $\Delta \log \frac{\Lambda j}{\Lambda_0} = 1$ for the RG scale parameterization $\Lambda_j = \Lambda_0 \exp(-j)$. We now redefine Kondo coupling as a dimensionless parameter

$$K^{(j)} = \frac{J^{(j)}}{\omega - \frac{\hbar v_F}{2}\Lambda_j}\ , \quad (13)$$

and operate in the regime $\omega > \frac{\hbar v_F}{2}\Lambda_j$. With the above parametrization of eq.(13), we can convert the difference RG relation (eq.(12)) into a continuum RG equation

$$\frac{dK}{d\log \frac{\Lambda}{\Lambda_0}} = \left(1 - \frac{\omega}{\omega - \hbar v_F \Lambda}\right) K + \frac{n(\Lambda)K^2}{1 - \frac{K^2}{16}} \quad (14)$$

Upon approaching the Ferm surface $\Lambda_j \to 0$, $\left(1 - \frac{\omega}{\omega - \hbar v_F \Lambda}\right) \to 0$ and $n(\Lambda)$ can be replaced by density of states on the Fermi surface $n(0)$:

$$\frac{dK}{d\log \frac{\Lambda}{\Lambda_0}} = \frac{n(0)K^2}{1 - \frac{K^2}{16}} \quad (15)$$

At this point, we observe an important aspect of the RG equation: for $K << 1$, the

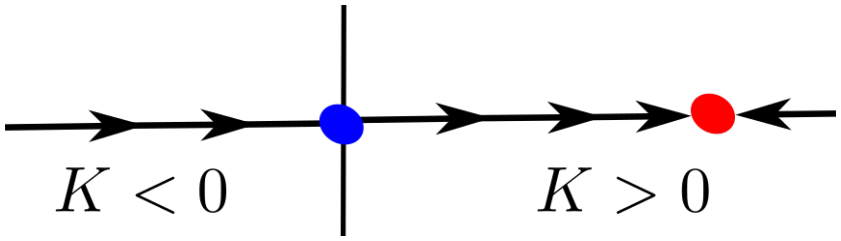

FIG. 3. Schematic RG phase diagram for the Kondo problem. The red dot represents intermediate coupling fixed point at $K^* = 4$ for the case of the AFM Kondo coupling. The blue dot represents the critical fixed point at $K^* = 0$ for the case of the FM Kondo coupling.

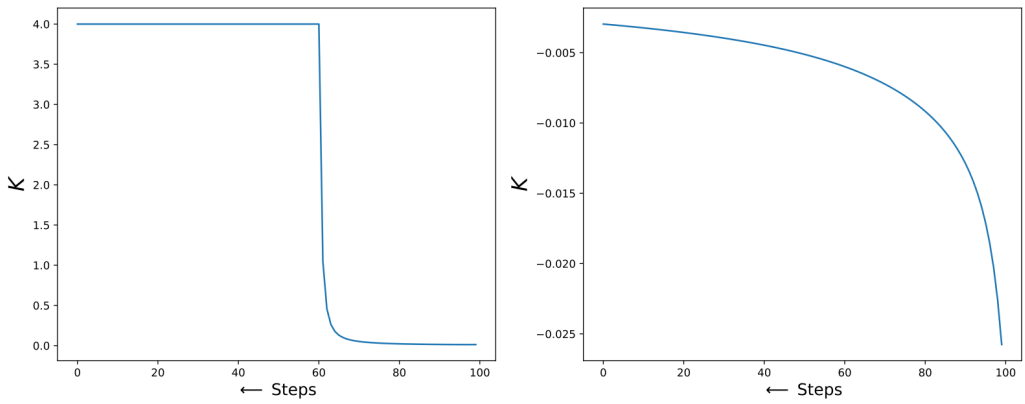

FIG. 4. Renormalized dimensionless Kondo coupling K with RG steps ($\log \Lambda_j/\Lambda_0$)for left panel: $K > 0$, and right panel: $K < 0$. The growth of the Kondo coupling to a finite value of the intermediate coupling fixed point is evident in the left panel, while the decay to zero at the critical fixed point can be seen in the right panel.

RG equation reduces to the one loop form: $\frac{dK}{d\log\frac{\Lambda}{\Lambda_0}} = K^2$ [2]. On the other hand, the nonperturbative form of the flow equation obtained from the URG formalism shows the presence of intermediate coupling fixed point at $K^* = 4$ in the antiferromagnetic regime $K > 0$. Upon integrating the RG equation and using the fixed point value $K^* = 4$ we obtain the Kondo energy scale (T_K) and thence the effective length of the Kondo cloud (ξ_K)

$$\begin{aligned}
&\frac{1}{K_0} - \frac{1}{2} + \frac{K_0}{16} = -n(0)\log\frac{\Lambda^*}{\Lambda_0}\ , \\
&\Lambda^* = \Lambda_0 \exp\left(\frac{1}{2n(0)} - \frac{1}{n(0)K_0} - \frac{K_0}{n(0)16}\right)\ , \\
&T_K = \frac{\hbar v_F \Lambda^*}{k_B} = \frac{\hbar v_F \Lambda_0}{k_B}\exp\left(\frac{1}{2n(0)} - \frac{1}{n(0)K_0} - \frac{K_0}{n(0)16}\right)\ , \\
&\xi_K = \frac{2\pi}{\Lambda^*} = \frac{hv_F}{k_B T_K} = \frac{2\pi}{\Lambda_0}\exp\left(-\frac{1}{2n(0)} + \frac{1}{n(0)K_0} + \frac{K_0}{n(0)16}\right)\ .
\end{aligned} \tag{16}$$

At the IR fixed point in the AF regime the effective Hamiltonian is given by,

$$H^* = \sum_{|\Lambda|<\Lambda^*} \hbar v_F \Lambda \hat{n}_{\Lambda,\hat{s},\sigma} + \frac{J^*}{2} \sum_{\substack{j_1,j_2<j^*,\\ m,m'}} \mathbf{S}\cdot c^\dagger_{j_1,\hat{s}_m,\alpha}\boldsymbol{\sigma}_{\alpha\beta}c_{j_2,\hat{s}_{m'},\beta} + \sum_{j'=N,m=1}^{j^*,n_{j'}} J^{j'} S^z s^z_{j',m} \tag{17}$$

AMHere m refers to the various normal directions $\hat{s}_m$ of the Fermi surface.AM In the above equation, the second term is the effective Hamiltonian for the coupling of the Kondo cloud to the impurity spin, while the third encodes the interaction between the impurity

spin moment and the decoupled electronic degrees of freedom that do not belong to the Kondo cloud (lying on radial shells in momentum-space indexed by the RG step j). When taken together with the first term (the kinetic energy/dispersion of the lattice conduction electrons), the third gives rise to the local Fermi liquid of Nozieres as it can be viewed as a self-energy for the decoupled electrons in the j' shell arising from their interaction with the impurity spin

$$\Sigma_{j'}^{dec} = J^{j'} \langle S^z \rangle \ . \tag{18}$$

As shown in Fig.4 (left panel), the local nature of the Fermi liquid can be seen by the rapid rise of the coupling $J^j = 2K_j\epsilon_j$ with RG step/shell index j only very near to where the Kondo coupling saturates (signalling the Kondo cloud formation).

We can now extract a zero mode from the above Hamiltonian that captures the low energy theory near the Fermi surface,

$$\begin{aligned} H_{coll} &= \frac{1}{N} \sum_{|\Lambda|<\Lambda^*} \hbar v_F \Lambda \sum_{|\Lambda|<\Lambda^*} \hat{n}_{\Lambda,\hat{s},\sigma} + \frac{J^*}{2} \sum_{\substack{j_1,j_2<j^*, \\ m,m'}} \mathbf{S} \cdot c^\dagger_{j_1,\hat{s}_m,\alpha} \boldsymbol{\sigma}_{\alpha\beta} c_{j_2,\hat{s}_{m'},\beta} + \sum_{j'=N,m=1}^{j,n_{j'}} J^{j'} S^z s^z_{j',m} \\ &= \frac{J^*}{2} \sum_{\substack{j_1,j_2<j^*, \\ m,m'}} \mathbf{S} \cdot c^\dagger_{j_1,\hat{s}_m,\alpha} \boldsymbol{\sigma}_{\alpha\beta} c_{j_2,\hat{s}_{m'},\beta} + \sum_{j'=N,m=1}^{j^*,n_{j'}} J^{j'} S^z s^z_{j',m} \ , \end{aligned} \tag{19}$$

where the first term vanishes as the sum over wavevector Λ within the symmetric window Λ^* around the Fermi surface itself vanishes.

Indeed, we observe that the zero mode Hamiltonian at the IR fixed point is responsible for the formation of the Kondo singlet ground state

$$|\Psi*\rangle = \frac{1}{\sqrt{2}} \left[|\uparrow\rangle \sum_{\Lambda,\hat{s}} |1_{\Lambda,\hat{s},\downarrow}\rangle \otimes_{\Lambda'\neq\Lambda,\hat{s}'\neq\hat{s}} |\Lambda',\hat{s}'\rangle - |\downarrow\rangle \sum_{\Lambda,\hat{s}} |1_{\Lambda,\hat{s},\uparrow}\rangle \otimes_{\Lambda'\neq\Lambda,\hat{s}'\neq\hat{s}} |\Lambda',\hat{s}'\rangle \right] \ . \tag{20}$$

Note that this state will be in direct product with the wavefunction for the decoupled electronic degrees of freedom.

Variation of the Kondo cloud size ξ_K and effective Kondo coupling J^* as function of bare coupling J_0

In Figs. 5, 6 and 7, we shown the variation of the Kondo cloud size ξ_K and effective Kondo coupling J^* as function of bare coupling J_0 (in units of t) in the weak ($4.9 \times 10^{-3} <$

$J < 7 \times 10^{-3}$), intermediate ($1 < J < 10$) and all the way till the strong coupling regime ($4.9 \times 10^{-3} < J < 10^7$) respectively. All plots below are obtained for momentum space grid 100×100 and with RG scale factor $\Lambda_j = b\Lambda_{j+1}$ ($b = 0.9999 = 1 - 1/N * N$, $N = 100$). The E_F for the 2d tight binding band $-W/2 < E_k = -2t(\cos k_x + \cos k_y) < W/2$ ($W = 4t$) is chosen at $E_F = -3.8t$.

While the variations of ξ_K in the weak and intermediate coupling regimes of J_0 (Fig. 5 and 6) are consistent with the result expected from a 1-loop RG calculation, it clearly shows that ξ_K saturates at the final RG step (corresponding to the Kondo cloud formation) at strong coupling (Fig.7). Similarly, J^* is consistent with the expectations from a 1-loop RG coupling at weak coupling (Fig.5), shows a tendency towards saturation in the intermediate coupling regime (Fig.6) and clearly saturates to a very large (strong coupling) value ($J^*_{sat} = 1.24 \times 10^4$, Fig.7) for $10 < J_0 < 10^7$. We recall that Wilson's NRG calculation for the Kondo problem (for a bath of conduction electrons in the continuum with linear dispersion and a very large UV cutoff D) shows that the renormalised Kondo coupling $J \to \infty$ under flow to strong coupling. This can be reconciled from our URG results by noting that that the value of J^*_{sat} increases upon rescaling the conduction bath bandwidth D to larger values (by rescaling the nearest neighbour hopping strength t). This is shown in Fig.8, where we see that J^*_{sat} increases from a value of the order of 10^4 (in units of t) to 10^{10} as t is increased from order 1 to 10^6. Thus, taking the limit of $D \to \infty$ will lead to $J^*_{sat} \to \infty$.

IMPURITY SPIN SUSCEPTIBILITY AND SPECIFIC HEAT CALCULATION FOR THE KONDO HAMILTONIAN

The effective Hamiltonian obtained at the IR fixed point eq.(17) commutes with the z-component of the net spin vector,

$$S^z_{tot} = S^z + \sum_{\substack{\Lambda,\Lambda'<\Lambda^*,\\ m,m'\\ \alpha,\beta}} c^\dagger_{\Lambda,\hat{s}_m,\alpha} \frac{\sigma^z_{\alpha\beta}}{2} c_{\Lambda',\hat{s}_{m'},\beta} + \sum_{\Lambda \geq \Lambda^*,m} s^z_{\Lambda,m}, \quad s^z_{\Lambda,m} = \frac{1}{2}\left(\hat{n}_{\Lambda,\hat{s}_m,\uparrow} - \hat{n}_{\Lambda,\hat{s}_m,\downarrow}\right) \ . \quad (21)$$

$$[H^*, S^z_{tot}] = 0 \quad (22)$$

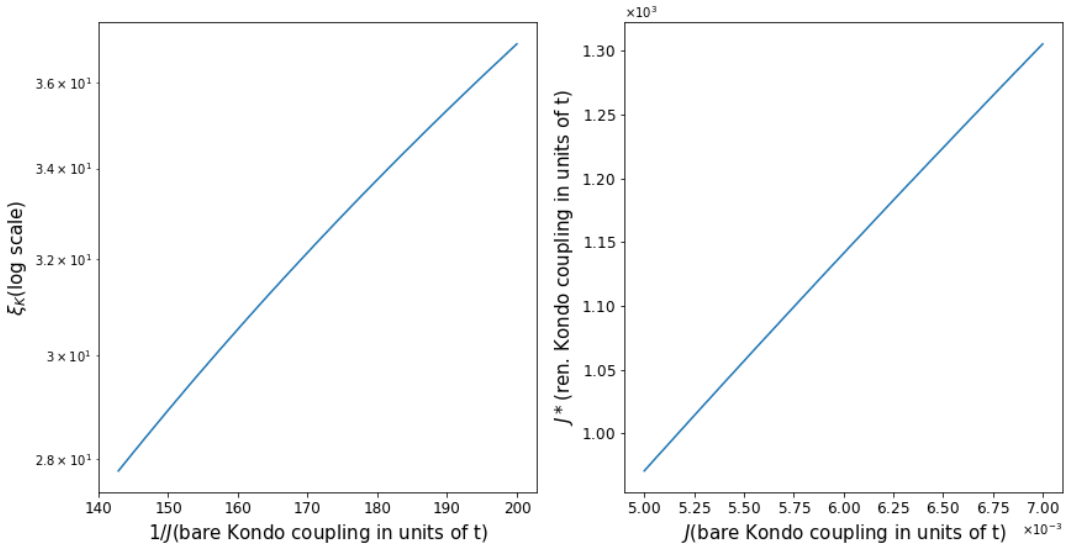

FIG. 5. Left panel: Kondo cloud length ξ in log scale (y-axis) vs. $1/J_0$ (x-axis), right panel: renormalized Kondo coupling J^* vs. J_0, for $5 \times 10^{-3}t < J_0 < 7 \times 10^{-3}t$.

The spin susceptibility originating purely from the impurity at the IR fixed originating simply from the impurity can be defined as,

$$\chi(T) = \frac{1}{kT}\left[\frac{Tr((S^z_{tot})^2 \exp(-H^*(0)/kT)}{Tr(\exp(-H^*(J^*)/kT))} - \left(\frac{Tr((S^z_{tot})^2 \exp(-H^*(0)/kT)}{Tr(\exp(-H^*(J^*)/kT))} - \frac{1}{4}\right)\right] \tag{23}$$

Since the eigenvalues of S^z_{tot} are good quantum nos for the eigenstates of H^* we can use those states to obtain these quantity. Similar thing can be done for the specific heat. The second term in the above expression cancels of the contribution coming to susceptibility from conduction electrons at $J^* = 0$. The final term $1/4$ cancels of the impurity susceptibility from $J^* = 0$ term. This prescription is due to Wilson [5].

TENSOR NETWORK REPRESENTATION OF THE KONDO URG PROGRAM

In this section, we present the tensor network representation of the URG program [4, 6]. The yellow blocks represent the complete unitary transformation $U_{(j)}$ for a given RG step composed of individual $U_{j,l}$ unitary operators that disentangle one electronic state $\mathbf{k}_{\Lambda\hat{s}}, \sigma$ each. The wavefunction $|\Psi^*\rangle$ comprises the IR bulk of the tensor network. The yellow layers are arranged along the RG direction. The tensor network Fig.9 is composed of yellow

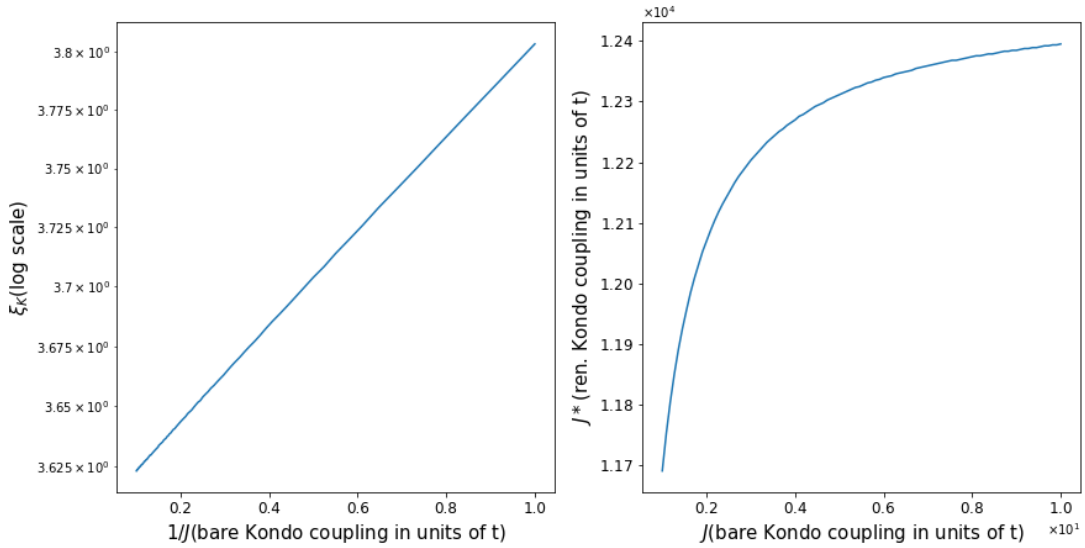

FIG. 6. Left panel: Kondo cloud length ξ in log scale (y-axis) vs. $1/J_0$ (x-axis), right panel: renormalized Kondo coupling J^* vs. J_0, for $t < J_0 < 10t$.

layers that lead to a holographic arrangement of eigenstates from UV to IR. As outlined in Fig.(10), by starting from the singlet state obtained at RG fixed point, we can perform the inverse unitary map to regenerate the entanglement with UV degrees of freedom. This enables us in obtaining the complete form of the many-particle wavefunction, and thence the two-point retarded Green's function, along the RG flow direction (RG time) $\tau_j = 1/v_F\Lambda_j$

$$G(\mathbf{k}\sigma,\tau;\mathbf{k}'\sigma',\tau') = \Theta(\tau-\tau')\langle\Psi_0|\{c_{\mathbf{k}\sigma}(\tau)c^\dagger_{\mathbf{k}'\sigma'}(\tau')\}|\Psi_0\rangle \ , \tag{24}$$

where $|\Psi_0\rangle = U_N^\dagger \dots U_{j^*}^\dagger|\Psi_{(j^*)}\rangle$ is the many-body state residing at the UV boundary of the tensor network. The many-body rotated $c^\dagger$, c operators are given by

$$c^\dagger_{\mathbf{k}'\sigma'}(\tau') = [U_j \dots U_N]c^\dagger_{\mathbf{k}'\sigma'}[U_j \dots U_N]^\dagger \ . \tag{25}$$

From the equal-time Green's function $G(\mathbf{k}\sigma,\tau;\mathbf{k}'\sigma',\tau)$, we can obtain the complete one-particle self-energy. From this, we can compute the spectral function, lifetime, quasiparticle residue etc. Importantly, this quantity is also related to mutual information or entanglement content between a pair of electronic states. This quantity will enable a simultaneous study of the quantum liquid comprising the Kondo cloud from both the many-body and quantum information theoretic perspectives. Indeed, a study of the many-particle entanglement Mott liquid in the 2D Hubbard model at 1/2-filling has already been carried out using a similar

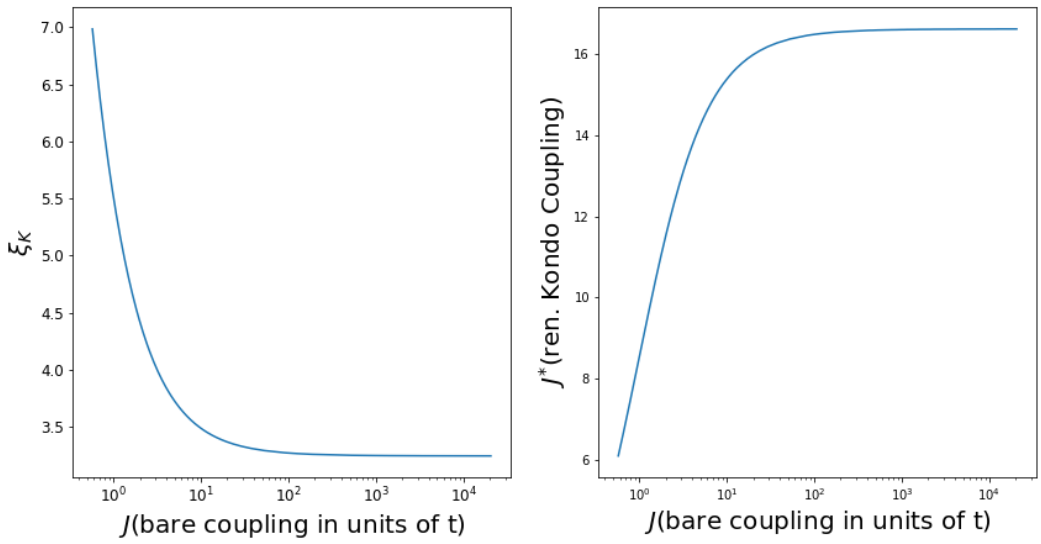

FIG. 7. Left panel: Kondo cloud length ξ vs. J_0 (x-axis in log scale) in , right panel: renormalized Kondo coupling J^* vs. J_0. J_0 is chosen as $4.9 \times 10^{-3} \times (1.02656)^n$ and $1 < n < 1000$.

reverse RG formulation [6]. We now seek to unite this strategy with standard Green's function techniques in the present work.

APPENDIX A: CALCULATION OF EFFECTIVE HAMILTONIAN FROM URG

Starting from the Kondo Hamiltonian eq.(1) and using the URG based Hamiltonian RG equation eq.(10) we obtain,

$$\begin{aligned}
\Delta\hat{H}_{(j)} = & \sum_{\substack{m=1,\\ \beta=\uparrow/\downarrow}}^{n_j} \frac{(J^{(j)})^2 \tau_{j,\hat{s}_m,\beta}}{2(2\omega\tau_{j,\hat{s}_m,\beta} - \epsilon_{j,l}\tau_{j,\hat{s}_m,\beta} - J^{(j)} S^z s^z_{j,\hat{s}_m})} \\
& \times \left[S^a S^b \sigma^a_{\alpha\beta}\sigma^b_{\beta\gamma} \sum_{\substack{(j_1,j_2<j),\\ n,o}} c^\dagger_{j_1,\hat{s}_n,\alpha} c_{j_2,\hat{s}_o,\gamma}(1-\hat{n}_{j,\hat{s}_m,\beta}) + S^b S^a \sigma^b_{\beta\gamma}\sigma^a_{\alpha\beta} \sum_{\substack{(j_1,j_2<j),\\ n,o}} c_{j_2,\hat{s}_o,\gamma} c^\dagger_{j_1,\hat{s}_n,\alpha} \hat{n}_{j,\hat{s}_m,\beta} \right] \\
& + \sum_{\substack{m=1,\\ \beta=\uparrow/\downarrow}}^{n_j} \frac{(J^{(j)})^2}{2(2\omega\tau_{j,\hat{s}_m,\beta} - \epsilon_{j,l}\tau_{j,\hat{s}_m,\beta} - J^{(j)} S^z s^z_{j,\hat{s}_m})} \left[S^x S^y \sigma^x_{\alpha\beta}\sigma^y_{\beta\alpha} c^\dagger_{j,\hat{s}_m,\alpha} c_{j,\hat{s}_m,\beta} c^\dagger_{j,\hat{s}_m,\beta} c_{j,\hat{s}_m,\alpha} \right. \\
& \left. + S^y S^x \sigma^x_{\alpha\beta}\sigma^y_{\beta\alpha} c^\dagger_{j,\hat{s}_m,\beta} c_{j,\hat{s}_m,\alpha} c^\dagger_{j,\hat{s}_m,\alpha} c_{j,\hat{s}_m,\beta} \right] \qquad (26)
\end{aligned}$$

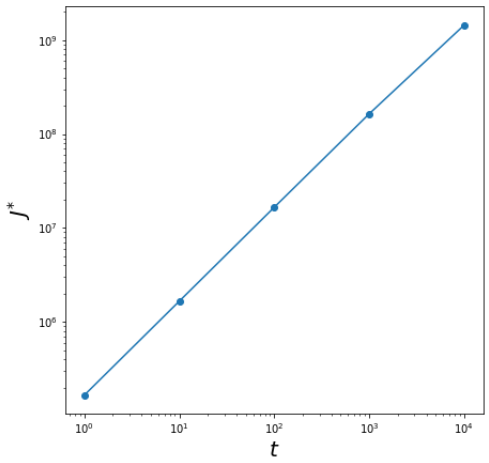

FIG. 8. Left panel: Variation of the renormalized Kondo coupling J^* with the hopping parameter t of the electronic bath t J_0, and hence the conduction band width. is varied J_0 is chosen as $4.9 \times 10^{-3} \times (1.02656)^n$ and $1 < n < 1000$.

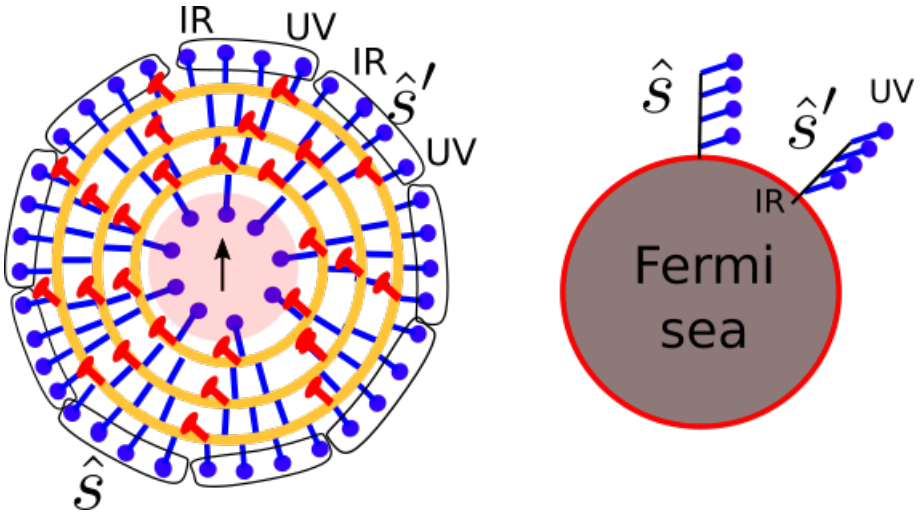

FIG. 9. Figure on the left shows a tensor network representation of the Kondo RG with 8 Fermi surface patches. The 32 blue nodes represents the 8 (for 8 $\hat{s}$) sets of 4(along a given normal $\hat{s}$) electronic states (qubits). arranged from UV to IR (see figure in the right). The yellow circular block represents the unitary gate that disentangles at each RG step 8 electronic qubits at UV. The red nodes represents the disentangled qubits comprising the bulk of the tensor network. At the IR bulk of the tensor network the pink circle represents the Kondo cloud coupling with the spin vector (up arrow).

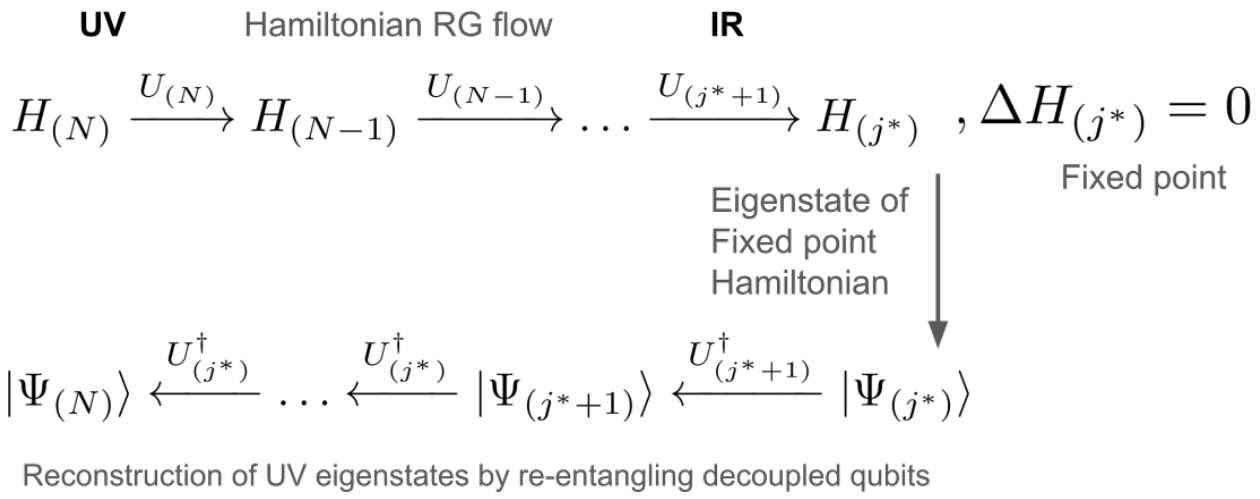

FIG. 10. The first line represent the Hamiltonian RG flow via the unitary maps. Upon reaching the Kondo IR fixed point, reverse RG will re-entangled decoupled electronic states with the Kondo singlet. This will result in generation of the many body eigenstates at UV.

The first term corresponds to the renormalization of the Kondo coupling and describes the sd-exchange interactions for the entangled degrees of freedom,

$$\begin{aligned}
\Delta H^1_{(j)} &= \sum_{\substack{m=1,\\ \beta=\uparrow/\downarrow}}^{n_j} \frac{(J^{(j)})^2 \tau_{j,\hat{s}_m,\beta}}{(2\omega\tau_{j,\hat{s}_m,\beta} - \epsilon_{j,l}\tau_{j,\hat{s}_m,\beta} - J^{(j)} S^z s^z_{j,\hat{s}_m})} \mathbf{S}\cdot c^\dagger_{j,\hat{s}_m,\alpha} \frac{\boldsymbol{\sigma}_{\alpha\beta}}{2} c_{j,\hat{s}_m,\beta} \\
&= \frac{1}{2} \sum_{\substack{m=1,\\ \beta=\uparrow/\downarrow}}^{n_j} \frac{(J^{(j)})^2 \left[(\frac{\omega}{2} - \frac{\epsilon_{j,l}}{4}) + \frac{J^{(j)}}{2} S^z \tau_{j,\hat{s}_m,\beta} (\tau_{j,\hat{s}_m,\uparrow} - \tau_{j,\hat{s}_m,\downarrow}) \right]}{(\omega - \frac{\epsilon_{j,l}}{2})^2 - \frac{\left(J^{(j)}\right)^2}{16}} \\
&= \frac{n_j (J^{(j)})^2 \left[(\omega - \frac{\epsilon_j}{2}) \right]}{(\omega - \frac{\epsilon_{j,l}}{2})^2 - \frac{\left(J^{(j)}\right)^2}{16}} \mathbf{S}\cdot \sum_{\substack{(j_1,j_2<j),\\ n,o}} c^\dagger_{j_1,\hat{s}_n,\alpha} \frac{\boldsymbol{\sigma}_{\alpha\gamma}}{2} c_{j_2,\hat{s}_o,\gamma}
\end{aligned} \tag{27}$$

In obtaining the last step of the calculation we have assumed $\epsilon_{j,l} = \epsilon_j$ for a circular Fermi surface geoemetry. The renormalization of the number diagonal Hamiltonian for the imme-

diately disentangled electronic states $|j,\hat{s}_m,\sigma\rangle$ has the form,

$$\Delta H^2_{(j)} = \sum_{\substack{m=1,\\ \beta=\uparrow/\downarrow}}^{n_j} \frac{(J^{(j)})^2}{(2\omega\tau_{j,\hat{s}_m,\beta} - \epsilon_{j,l}\tau_{j,\hat{s}_m,\beta} - J^{(j)}S^z s^z_{j,\hat{s}_m})} \Big[S^x S^y \sigma^x_{\alpha\beta}\sigma^y_{\beta\alpha} c^\dagger_{j,\hat{s}_m,\alpha} c_{j,\hat{s}_m,\beta} c^\dagger_{j,\hat{s}_m,\beta} c_{j,\hat{s}_m,\alpha}$$
$$+ S^y S^x \sigma^x_{\alpha\beta}\sigma^y_{\beta\alpha} c^\dagger_{j,\hat{s}_m,\beta} c_{j,\hat{s}_m,\alpha} c^\dagger_{j,\hat{s}_m,\alpha} c_{j,\hat{s}_m,\beta} \Big]$$
$$= \sum_{\substack{m=1,\\ \beta=\uparrow/\downarrow}}^{n_j} \frac{(J^{(j)})^2}{(2\omega\tau_{j,\hat{s}_m,\beta} - \epsilon_{j,l}\tau_{j,\hat{s}_m,\beta} - J^{(j)}S^z s^z_{j,\hat{s}_m})} S^z \frac{\sigma^z_{\alpha\alpha}}{2} \Big[\hat{n}_{j,\hat{s}_m,\alpha}(1-\hat{n}_{j,\hat{s}_m,\beta}) - \hat{n}_{j,\hat{s}_m,\beta}(1-\hat{n}_{j,\hat{s}_m,\alpha}) \Big]$$
$$= \sum_{m=1}^{n_j} \frac{(J^{(j)})^2}{(2\omega\tau_{j,\hat{s}_m,\beta} - \epsilon_{j,l}\tau_{j,\hat{s}_m,\beta} - J^{(j)}S^z s^z_{j,\hat{s}_m})} S^z s^z_{j,\hat{s}_m} \tag{28}$$

in the last step we have used $\hat{n}_{j,\hat{s}_m,\alpha}(1-\hat{n}_{j,\hat{s}_m,\beta}) - \hat{n}_{j,\hat{s}_m,\beta}(1-\hat{n}_{j,\hat{s}_m,\alpha}) = \hat{n}_{j,\hat{s}_m,\alpha} - \hat{n}_{j,\hat{s}_m,\beta}$and the spin density for the state $|j,\hat{s}_m\rangle$ is given by $s^z_{j,\hat{s}_m} = \frac{1}{2}(\hat{n}_{j,\hat{s}_m,\uparrow} - \hat{n}_{j,\hat{s}_m,\downarrow})$.

In obtaining the above RG equation we have replaced $\hat{\omega}_{(j)} = 2\omega\tau_{j,\hat{s}_m,\beta}$. We set the electronic configuration $\tau_{j,\hat{s}_m,\uparrow} = +\tau_{j,\hat{s}_m,\downarrow} = -\frac{1}{2}$ to account for the spin scattering between the Kondo impurity and the fermionic bath. The operator $\hat{\omega}_{(j)}$ (eq.(7)) for RG step j is determined by the occupation number diagonal piece of the Hamiltonian $H^D_{(j-1)}$ attained at the next RG step $j-1$, this demands a self consistents treatment of the RG equation to determine the ω. In this fashion two particle and higher order quantum fluctuations autamatically get encoded into the RG dynamics of $\hat{\omega}$. In the present work we restrict our study by ignoring the RG contribution in ω. The electron/hole configuration ($|1_{j,\hat{s}_m,\beta}\rangle/|0_{j,\hat{s}_m,\beta}\rangle$) of the disentangled electronic state and associated with $\pm\epsilon_{j,l}$ energy is accounted by $\pm\omega$ fluctuation energy scales. From the above Hamiltonian RG equations eq.(27) we can obtain the form of the Kondo coupling RG equations,

$$\Delta J^{(j)} = \frac{n_j (J^{(j)})^2 \left[(\frac{\epsilon_{j,l}}{2} - \omega) \right]}{(\frac{\epsilon_{j,l}}{2} - \omega)^2 - \frac{\left(J^{(j)}\right)^2}{16}} \ . \tag{29}$$

APPENDIX B: DERIVATION OF THE LOCAL FERMI LIQUID THEORY FROM EFFECTIVE HAMILTONIAN

$$H_{coll} = J^* \mathbf{S}\cdot\mathbf{s} + \sum_{l=N,m=1}^{j^*,n_l} J_l S^z s^z_{l,m} + \sum_{l=N,m=1}^{j^*,n_l} \epsilon_l (\hat{n}_{l,m,\uparrow} + \hat{n}_{l,m,\downarrow}) \tag{30}$$

$$\rho = \exp(-\beta H_K^*) = \prod_{l=N,m=1}^{j^*,n_l} \exp(-\beta\epsilon_l(\hat{n}_{l,m,\uparrow} + \hat{n}_{l,m,\downarrow})) \times \exp(-\beta(J^*\mathbf{S}\cdot\mathbf{s} + \sum_{l=N,m=1}^{j^*,n_l} J_l S^z s^z_{l,m})) \quad (31)$$

Representing H_K^* in the $|\uparrow\downarrow\rangle$ and $|\downarrow\uparrow\rangle$ basis of the impurity spin and Kondo cloud.

$$\begin{pmatrix} -\frac{J^*}{4} + \sum_{l=N,m=1}^{j^*,n_l} \frac{J_l}{2} s^z_{l,m} & \frac{J^*}{2} \\ \frac{J^*}{2} & -\frac{J^*}{4} - \sum_{l=N,m=1}^{j^*,n_l} \frac{J_l}{2} s^z_{l,m} \end{pmatrix} = -\frac{J^*}{4} + \sigma^z h_z + \frac{J^*}{2}\sigma_x = -\frac{J^*}{4} + A\boldsymbol{\sigma}\cdot\hat{\mathbf{n}},$$

$$A = \sqrt{h_z^2 + \frac{(J^*)^2}{4}}, \cos\theta = \frac{h_z}{\sqrt{h_z^2 + \frac{(J^*)^2}{4}}}, h_z = \sum_{l=N,m=1}^{j^*,n_l} \frac{J_l}{2} s^z_{l,m} \quad (32)$$

$$\begin{aligned} &\exp(-\beta(J^*\mathbf{S}\cdot\mathbf{s} + \sum_{l=N,m=1}^{j^*,n_l} J_l S^z s^z_{l,m})) \\ &= 2\exp(-\beta\frac{J^*}{4})\cosh\left(\sum_{l=N,m=1}^{j^*,n_l} \frac{\beta J_l}{2} s^z_{l,m}\right) + \exp(\beta\frac{J^*}{4})\exp\left(-\beta A\sigma\cdot\hat{\mathbf{n}}\right) \\ &= 2\exp(-\beta\frac{J^*}{4})\cosh\left(\sum_{l=N,m=1}^{j^*,n_l} \frac{\beta J_l}{2} s^z_{l,m}\right) + \exp(\beta\frac{J^*}{4})\left[\cosh(\beta A) + \boldsymbol{\sigma}\cdot\hat{n}\sinh(\beta A)\right] \quad (33) \end{aligned}$$

$$Tr_{imp+cloud}(\exp(-\beta(J^*\mathbf{S}\cdot\mathbf{s} + \sum_{l=N,m=1}^{j^*,n_l} J_l S^z s^z_{l,m}))) \approx \exp(\beta\frac{J^*}{4})\exp(\beta A), \text{ for } \beta\to\infty \quad (34)$$

$$\begin{aligned} H_{eff} = -k_B T\log(Tr_{imp+cloud}(\exp(-\beta H_K^*)) &\approx \sum_{l,m}\epsilon_l(\hat{n}_{l,m,\uparrow} + \hat{n}_{l,m,\downarrow}) - \frac{J^*}{4} - \frac{J^*}{2}\sqrt{1 + \frac{4h_z^2}{(J^*)^2}} \\ &\approx \sum_{l,m}\epsilon_l(\hat{n}_{l,m,\uparrow} + \hat{n}_{l,m,\downarrow}) - \frac{3J^*}{4} - \frac{h_z^2}{J^*} \quad (35) \end{aligned}$$

Upon expanding the square root term in H_{eff} in leading orders of $\frac{h^z}{J^*}$ we obtain the Fermi liquid at IR fixed point

$$H_{FL} = \sum_{l,m}\epsilon_l(\hat{n}_{l,m,\uparrow} + \hat{n}_{l,m,\downarrow}) - \sum_{l,l',m,m'} f_{ll'} s^z_{l,m} s^z_{l,m'}, f_{ll'} = \frac{J_l J_{l'}}{J^*}, s^z_{l,m} = \frac{1}{2}(\hat{n}_{l,m,\uparrow} - \hat{n}_{l,m,\downarrow}) \quad (36)$$

Given the interaction strength $f_{ll'} = \frac{J_l J_{l'}}{J^*}$ falls off sharply compared to $\epsilon_{\Lambda*}$ with increasing distances $\Lambda > \Lambda^*$, the highest magnitude being $f_{j^*} = J_* = 4\epsilon_{\Lambda^*}$ for electronic states on shell Λ^* we obtain the local Fermi liquid Hamiltonian,

$$H_{LFL} = \epsilon_* \sum_m (\hat{n}_{*,m,\uparrow} + \hat{n}_{*,m,\downarrow}) - J^* \sum_{m,m'} s^z_{*,m} s^z_{*,m'}, s^z_{*,m} = \frac{1}{2}(\hat{n}_{\Lambda^*,m,\uparrow} - \hat{n}_{\Lambda^*,m,\downarrow}) \ . \quad (37)$$

Here m

APPENDIX C: OBTAINING WILSON RATIO FOR THE LOCAL FERMI LIQUID

$$\mathcal{E} = \mathcal{E}_0 + \epsilon_* \sum_{m,\sigma} \delta n_{*,m,\sigma} + \frac{J^*}{4} \sum_{m,m',\sigma} \delta n_{*,m,\sigma} \delta n_{*,m',-\sigma} + \frac{J^*}{4} \sum_{m,m',\sigma} n_{*,m,\sigma} \delta n_{*,m',-\sigma} \tag{38}$$

$$\begin{aligned} \frac{\delta \mathcal{E}}{\delta n_{*,m,\sigma}} &= \epsilon_* + \frac{J^*}{4} \sum_{m'} \delta n_{*,m',-\sigma} + \frac{J^*}{4} \sum_{m'} n_{*,m',-\sigma} \\ &= \epsilon_* + \frac{\Delta\epsilon}{\pi} \delta_\sigma(\{n_{*,m',-\sigma}\}, \epsilon_*) \end{aligned} \tag{39}$$

here we have taken

$$\begin{aligned} E_k - E_F &= -2t\cos(k_{Fx} + \Lambda^*) - 2t\cos(k_{Fy} + \Lambda^*) + 2t\cos k_{Fx} + 2t\cos k_{Fy} \\ &= 2t(\sin k_{Fx} + \sin k_{Fy})\Lambda^* \approx 2t(k_{Fx} + k_{Fy})\Lambda^* \end{aligned} \tag{40}$$

therefore,

$$\frac{\Delta E}{\Delta \Lambda^*} = 2t(k_{Fx} + k_{Fy}) \tag{41}$$

$$\Delta\epsilon = 2t(k_{Fx} + k_{Fy})\frac{\pi}{L} \tag{42}$$

$$\delta_\sigma(\{n_{*,m',-\sigma}\}, \epsilon_*) = \frac{\pi J^*}{4\Delta\epsilon} \sum_{m'} \delta n_{*,m',-\sigma} + \frac{\pi}{2} + \alpha(\epsilon_* - E_F) \tag{43}$$

where $\delta_0 = \frac{\pi}{2}$ is the phase shift accounting for the absorption of the Kondo cloud into the singlet. $\alpha(\epsilon^* - E_F) = \frac{\pi J^*}{4\Delta\epsilon} \sum_{m'} n_{*,m',-\sigma} - \frac{\pi}{2}$ accounts for the quasiparticle self energy generated by potential scattering with the impurity+cloud singlet[7–9]. Following Ref.[8, 9] we obtain the zero temperature specific heat coefficient (in units of $k_B = 1$),

$$\gamma = \frac{2\pi}{3}\alpha(\epsilon_* - E_F) \tag{44}$$

and the impurity spin susceptibility,

$$\chi = \frac{4\alpha(\epsilon_* - E_F)}{\pi} \tag{45}$$

This leads to Wilson's ratio,

$$R = \frac{\chi}{\gamma}\frac{\pi^2}{3} = 2 \tag{46}$$

APPENDIX D: IMPURITY SUSCEPTIBILITY AT FINITE TEMPERATURES

The complete effective Hamiltonian for the impurity spin ($\mathbf{S}$), Kondo cloud spin ($\mathbf{s}$) and the electrons that comprise the local Fermi liquid has the form,

$$H_2 = \epsilon_* \sum_{m,\sigma} \hat{n}_{*,m,\sigma} + J^* \mathbf{S} \cdot \mathbf{s} + J^* S^z \sum_m s^z_{*,m} \ . \tag{47}$$

The Hamiltonian H_2 has several conserved quantities which we depict below,

$$[H_2, S^z + s^z] = 0 \ , \ [H_2, s^z_{*,m}] = 0 \ \forall \ 1 \leq m \leq n_j \tag{48}$$

such that $[H^*, S^z_{tot}] = 0$ where $S^z_{tot} = S^z + s^z + \sum_m s^z_{*,m}$. Therefore the eigenvalues of $|s^z_{*,m} = \uparrow \ / \ \downarrow\rangle$ are good quantum numbers; this is simply an outcome of the URG method. We can now extract the effective Kondo impurity+ electron cloud Hamiltonian by treating the effect of local Fermi liquid electrons as an effective field $B = J^* \sum_m \langle s^z_{*,m} \rangle$ (note that this the eigenvalue of the LFL spins) on the impurity spin,

$$H^*_K = J^* \mathbf{S} \cdot \mathbf{s} + B S^z, \tag{49}$$

where we have treated the impurity spin density-density interaction ($\sum_m J^* S^z s^z_{*,m}$) energy cost $\frac{J^*}{4}$ for excitations of the local Fermi liquid lying above the ground state $E_g = -\frac{3J^*}{4}$. It is also important to note that the URG procedure did not lead to the generation of spin density density interaction between the electrons of the Kondo cloud and those of the LFL. We now obtain the impurity magnetization and susceptibility from this effective Hamiltonian. The eigenspectrum of H^*_K is given by,

$$E_1 = \frac{1}{2}(-\frac{J*}{2} + \sqrt{B^2 + J^{*2}}), E_2 = \frac{1}{2}(-\frac{J*}{2} - \sqrt{B^2 + J^{*2}}),$$
$$E_3 = E_4 = \frac{J*}{4} \tag{50}$$

The partition for this Hamiltonian for $\beta = \frac{1}{k_B T}$ is given by,

$$Z(B) = 2 \exp(\beta \frac{J*}{4}) \left[\cosh(\beta \frac{B}{2}) + \cosh(\frac{\beta}{2}(\sqrt{B^2 + J^{*2}})) \right] \tag{51}$$

The magnetization is given by,

$$M = \frac{k_B T}{Z(B)} \frac{dZ(B)}{dB} = \frac{k_B T}{Z(B)} \exp(\beta \frac{J*}{4}) \beta \left[\sinh(\beta \frac{B}{2}) + \frac{B}{\sqrt{B^2 + J^{*2}}} \sinh(\frac{\beta}{2} \sqrt{B^2 + J^{*2}}) \right] \tag{52}$$

The susceptibility is obtained by taking the effective field $B \to 0$,

$$\chi = \lim_{B\to 0} \frac{dM}{dB} = \frac{\frac{\beta}{4} + \frac{1}{2J^*}\sinh(\frac{\beta}{2}J^*)}{1+\cosh(\frac{\beta}{2}J^*)} \tag{53}$$

The saturation value of χ as $\beta \to \infty$ is given by,

$$\chi(T=0) = \frac{1}{2J^*} \ . \tag{54}$$

The Wilson number $W = 4T_k\chi(T=0) = \frac{2T_k}{J^*}$ from the present formulation. For values of $J^* \simeq 16.612t$ and $T_k \simeq 3.433t$ we obtain $W = 0.413$. Similarly the saturation value of χ for $\beta \to 0$ is given by,

$$k_B T\chi(T=\infty) = \frac{1}{4} \ . \tag{55}$$

The $T_k\chi$ vs temperature curve has a nonmonotic behaviour a maxima seen via the transcendental equation below,

$$\frac{d\chi}{d\beta} = \frac{1}{4} - \frac{1}{4}\frac{(1+\frac{2}{J^*\beta}\sinh\frac{\beta J^*}{2})(\frac{J^*\beta}{2}\sinh\frac{\beta J^*}{2})}{(1+\cosh\beta\frac{J^*}{2})^2} \implies (1+\cosh\beta\frac{J^*}{2})^2 = \frac{J^*\beta}{2}\sinh\frac{\beta J^*}{2} + \sinh^2\frac{\beta J^*}{2} \tag{56}$$

We numerically confirm that the maxima is obtained at $T \simeq T_k$.

* am14rs016@iiserkol.ac.in

† slal@iiserkol.ac.in

‡ raja@jncasr.in

§ arghya@phy.kgp.ernet.in

[1] J. Kondo, Resistance minimum in dilute magnetic alloys, Progress of theoretical physics **32**, 37 (1964).

[2] P. Anderson, A poor man's derivation of scaling laws for the kondo problem, Journal of Physics C: Solid State Physics **3**, 2436 (1970).

[3] A. Mukherjee and S. Lal, Scaling theory for mott-hubbard transitions-i: T=0 phase diagram of the 1/2-filled hubbard model, arxiv preprint arxiv:2004.06900 (2019).

[4] a. A. Mukherjee and S. Lal, Unitary renormalisation group for correlated electrons-i: a tensor network approach, arXiv preprint arXiv:2004.06897 (2020).

[5] K. G. Wilson, The renormalization group: Critical phenomena and the kondo problem, Rev. Mod. Phys. **47**, 773 (1975).

[6] A. Mukherjee and S. Lal, Holographic entanglement renormalisation of topological order in a quantum liquid, arXiv preprint arXiv:2003.06118 (2020).

[7] R. M. Martin, Fermi-surfae sum rule and its consequences for periodic kondo and mixed-valence systems, Physical Review Letters **48**, 362 (1982).

[8] P. Nozieres, A fermi-liquid description of the kondo problem at low temperatures, Journal of low température physics **17**, 31 (1974).

[9] P. Coleman, *Introduction to many-body physics* (Cambridge University Press, 2015) chapter:18.